11th IGTC
Dispatchable technology & innovations for a carbon-neutral society
10-11 October 2023, Brussels, Belgium
Paper ID Number: 17-IGTC23

OPTIMIZATION OF GAS TURBINE-BASED MICROGRIDS: AN AIRPORT CASE STUDY

Andrea Zelaschi[a], Lorenzo Pilotti[a], Alessandro F. Castelli[a], Maria M. Gambini[b], Giovanni Tonno[b], Giulio Betti[b,*], Emanuele Martelli[a,*]

[a]Politecnico di Milano, Via Lambruschini 4, 20154 Milano, Italy
[b] Baker Hughes, Via Felice Matteucci, 2 | 50127, Firenze | Italy
*corresponding authors: emanuele.martelli@polimi.it, giulio.betti@bakerhughes.com

ABSTRACT

Due to the requirement of reducing CO_2 emissions and achieving sustainability in the energy sector, it is essential to integrate renewable energy sources with controllable generators and energy storage systems into multi-energy systems. This study aims to optimize the design and operation of a multi-energy system for a medium-sized airport with high reliability requirements. The design of the system has been optimized with the code developed by Politecnico di Milano for aggregated energy systems (microgrids, energy districts, CHP systems, virtual power plants, etc). The code determines the optimal selection, sizing, and operation of units based on expected hourly energy demand profiles of the airport's users, PV production potential, costs, and performance curves of available generators. The code can include a wide range of reliability constraints (N-1 reliability, spinning reserve, etc.) and optimize the sizing and management of the electric vehicle charging infrastructure. The catalogue of units includes CHP gas turbines, heat pumps, PV, and battery and thermal energy storage systems. The study shows the effectiveness of the optimal design code in dealing with real-world problems.

INTRODUCTION

In recent years, policies aimed at reducing carbon dioxide (CO_2) emissions and the consumption of fossil fuels in the energy sector have been gaining momentum. According to the International Energy Agency (2021b) an immediate action is required to achieve the goal of net-zero emissions by 2050, which is necessary to limit global warming to 1.5°C above pre-industrial levels.

Solar energy (PV) and wind are the most commonly used renewable sources due to their availability and relatively low cost of electricity. However, the intermittent nature of these sources poses the need to install flexible dispatchable generators and/or energy storages to ensure a reliable energy supply.

In this context, Multi-energy systems (MES) and microgrids (MG), here called "Aggregated Energy Systems" (AES), are emerging as key elements of the future energy transition, being an effective solution to integrate distributed renewable energy sources (RES) with controllable generators and energy storage systems (IEA, 2017). These systems, which can operate both in grid-connected and islanded mode, can provide different energy vectors, such as electricity and heat, to the final users in a synergistic way, and can be used for a range of industrial and civil facilities, including airports, hospitals, and schools.

The rule of thumbs, design criteria and operating modes developed for conventional centralized energy systems are not applicable to multi-energy systems due to the elevated number of units involved, their potential interactions and the variety of possible configurations. Therefore, the optimal design and operation of microgrids needs to be addressed by using mathematical optimization techniques. Among these techniques, those based on mixed-integer linear programming (MILP) formulations represent the state of the art because of the following key advantages: (i) they can properly model the combinatorial nature of the problem (units selection and on/off operation), (ii) they can be solved using branch-and-bound solvers with proved global convergence properties, (iii) commercially available MILP solvers can solve large scale problems (with thousands of constraints and variables) within practical times. In the last ten years, Politecnico di Milano has developed a MILP-based code for the systematic design optimization of different types of aggregated energy systems.

For example, Zatti et al. (2017) proposed a three-stage stochastic MILP model to tackle the design of smart energy districts, which includes electricity and heat storage, conversion, and distribution systems, under uncertainty. Gabrielli et al. (2018) presented a novel MILP formulation for the optimal design and operation of multi-energy systems involving seasonal energy storage. Zatti et al. (2019b) optimized the design and operation of a multi-energy system for a multiple-site university campus using a new clustering approach named k-MILP. The method provides the typical and extreme days of the year, setting a

maximum tolerance on the integral of the load duration curves. Castelli et al. (2022) optimized the design and operation of a fully renewable multi-energy system minimizing the total annual cost. The investigated MES integrates H_2-fired combined cycles, PV panels, electrolyzers, batteries for short-term storage, and H_2 seasonal storage.

In a recent research project, the AES design optimization code developed by the GECOS group (Group of Energy Conversion Systems) of Politecnico di Milano has been applied to gas-turbine-based microgrids in collaboration with Baker Hughes. In particular, the project has investigated off-grid applications typical of the oil & gas industry with high reliability requirements, and industrial case studies. This work reports the application to the design of an aggregated energy system serving an airport with high reliability requirements. The objective is to find the optimal design which minimizes the total annual cost, including capital and operational costs, while ensuring reliable and continuous energy supply to the airport. The case study is designed to represent an average airport with electrical and thermal demand that serves about 71 million passengers annually and is located at middle latitudes with an annual average solar irradiance of approximately 1780 kWh/m^2. The airport is designed to receive and charge approx. 1.1 million electric vehicles per year with smart charging stations. The catalogue of generators includes combined heat and power (CHP) gas turbines. In addition, it can also install a variable-size heat pump, photovoltaic, and battery and thermal energy storage systems (BESS and TES). A schematic representation of the AES is reported in Figure 1. To have a N-1 reliability of the airport power supply, the AES must meet the airport's electrical demand in case of failure of one generator using proper spinning-reserve constraints and spare units installation. The MILP model allows for optimal sizing of the charging station while optimally scheduling the charge of the EVs, thus considering the potential for demand side management.

NOMENCLATURE

AES	Aggregated energy system
BESS	Battery energy storage system
BH	Baker Hughes
CHP	Combined Heat and Power
CRF	Capital recovery factor
EV	Electric vehicles
MG	Microgrid
MILP	Mixed-integer linear programming
MES	Multi-energy system
PV	Photovoltaic
RES	Renewable Energy Sources
SAM	System Advisor Model
SOC	State of Charge
TAC	Total Annual Cost
TES	Thermal Energy Storage

FORMULATION OF THE OPTIMIZATION PROBLEM AND SYSTEM ASSUMPIONS

The optimization problem is a two-stage stochastic program that combines two steps: (i) the design stage, where the decisions on the type and size of units are made and (ii) the operation stage, where the optimal scheduling of the set of units selected in the previous stage is evaluated, and units status (i.e. on/off) and operative loads are determined.

As for the time-variable yearly profiles, the electricity demand, which encompasses the airport services, has been found to have an average of 22.3 MW_e and a peak of 60 MW_e. The monthly average profiles used are those of the Incheon Airport located in Seoul (Baek et al., 2016). Furthermore, the PV production and ambient temperature profiles have been extracted from the System Advisor Model (SAM) database for the Incheon Airport in 2019 (NREL, 2020). On the other hand, the thermal heat demand yearly profile, which has a peak of 27.9 MW_{th}, has been estimated by multiplying the difference between the internal and external ambient temperature with an assumed proportionality constant. Additionally, the passenger arrival and departure profiles, utilized to calculate the EV arrival and departure schedule, have been assumed identical to those of the Incheon Airport in 2019. The representation of the time-variable yearly profiles is reported in Figure 2.

To reduce computational complexity, the AES operation is optimized for a representative subset of days, as the problem's complexity grows exponentially with the number of time steps. To identify these representative days, a k-medoids clustering algorithm is applied to the yearly profiles, considering a one-hour time step (Zatti et al., 2019b). Six "typical" days are selected for optimization purposes, which can adequately capture the system's behaviour under varying conditions. Each typical day represents a set of real days of the year. Additionally, to test the microgrid's robustness, the operation is also optimized for six "extreme" days that correspond to specific scenarios of interest, such as maximum and minimum hourly ambient temperature, maximum hourly PV production, minimum average daily PV production, and maximum peaks of electric and heat demand.

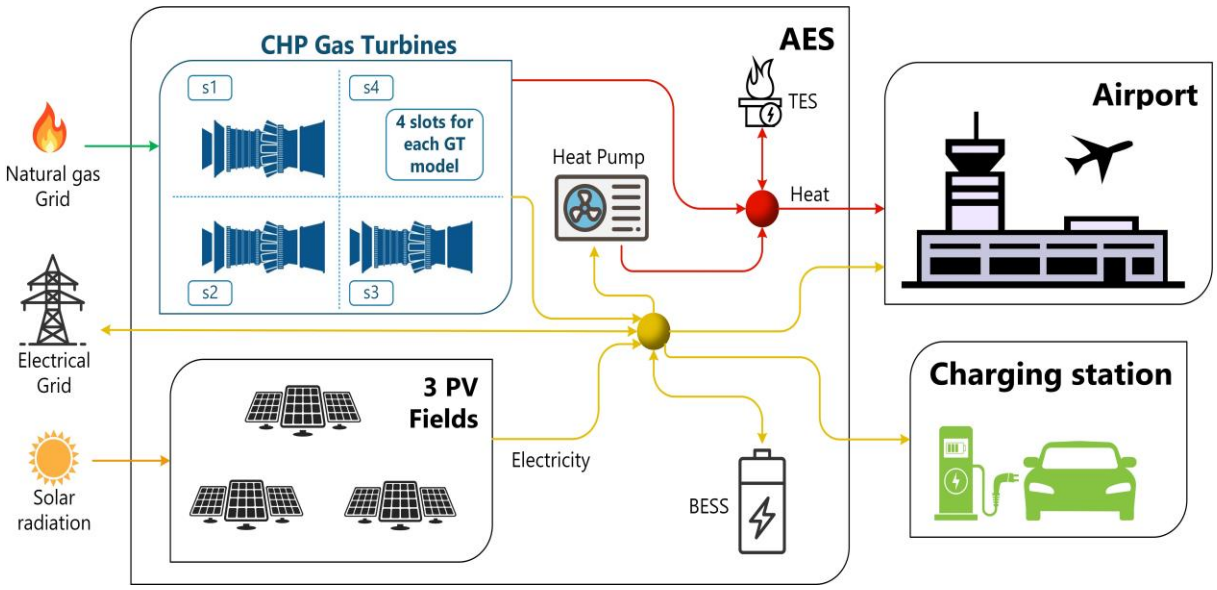

Figure 1. *Schematic representation of the investigated aggregated energy system.*

Problem Statement

The optimization problem can be stated as follows.

Given:

- The expected time-varying profiles of the energy demands (e.g. heat and electricity) over the optimization time horizon.
- The expected time-varying meteorological data (PV production and ambient temperature).
- The expected time-varying prices for purchasing and selling electricity (only in the grid-connected case).
- The expected costs of fuel and the carbon tax value.
- Performance and cost data of dispatchable units (CHP gas turbines and heat pump), storage systems (batteries and thermal energy storage), and not-dispatchable sources (PV).
- The expected lifetime and the relevant financial and economic parameters of the system.
- The limits on the flexible loads (EVs).

Determine the following decision variables:

- The dispatchable and not-dispatchable units and storages to install (1st stage decision).
- The optimal sizes of the selected units and storage systems (1st stage decision).
- The optimal size of the charging station (1st stage decision).
- The commitment status (i.e. on/off, start-up, showdown) of selected units (2nd stage decision).
- The optimal scheduling of units (i.e. generation/load, energy exchanges) in each timestep (2nd stage decision).
- The fuel and electricity power imported/exported (2nd stage decision).
- The optimal fraction of dispatchable loads (EVs) met in each time period (2nd stage decision).
- Storages management (i.e. charge/discharge power, energy level) in each timestep (2nd stage decision).

The objective is to minimize the total annual cost (TAC) while ensuring the energy balance and the other constraints. The TAC [$/y] is calculated as:

$$TAC = CRF \cdot \sum C_{inv} + \sum C_{O\&M}^{fix} + \sum_{sc=1}^{12} \tilde{\pi}_{SC} \cdot \left(C_{O\&M,sc}^{var} + C_{fuel,sc} + C_{Carbon_{tax},sc} + C_{grid,sc}^{purchase} + - R_{grid,sc}^{export}\right) \quad (1)$$

Where CRF is the capital recovery factor, assumed equal to 10%. C_{inv} is the investment cost of the installed units [$]. $C_{O\&M}^{fix}$ and $C_{O\&M}^{var}$ represent the fixed and variable O&M costs, respectively. $C_{O\&M}^{var}$, expressed in [$/day], also includes the start-up cost of the generators. $\tilde{\pi}_{SC}$ indicates the occurrence probability associated with each scenarios sc ("typical" and "extreme" days). The six clustered "typical" days have an occurrence which depends on how many real days belong to their cluster, while the six "extreme" days occur only once a year. $C_{fuel,sc}$ and $C_{Carbon_{tax},sc}$ represent the cost associated to the fuel expenses and the carbon tax, respectively. Lastly, $C_{grid,sc}^{purchase}$ denotes the cost for the electricity imported from the grid, while $R_{grid,sc}^{export}$ stands for the revenue for the electricity sold to the grid.

Modelling of the components

This section will present the main assumptions and how the installable units in the catalogue have been modelled.

CHP Gas Turbines

Five gas turbine models, named GTurbA, GTurbB, GTurbC, GTurbD and GTurbE, with data taken from commercial software, have been selected to represent five different general categories of generators in terms of nominal power, efficiency and costs.

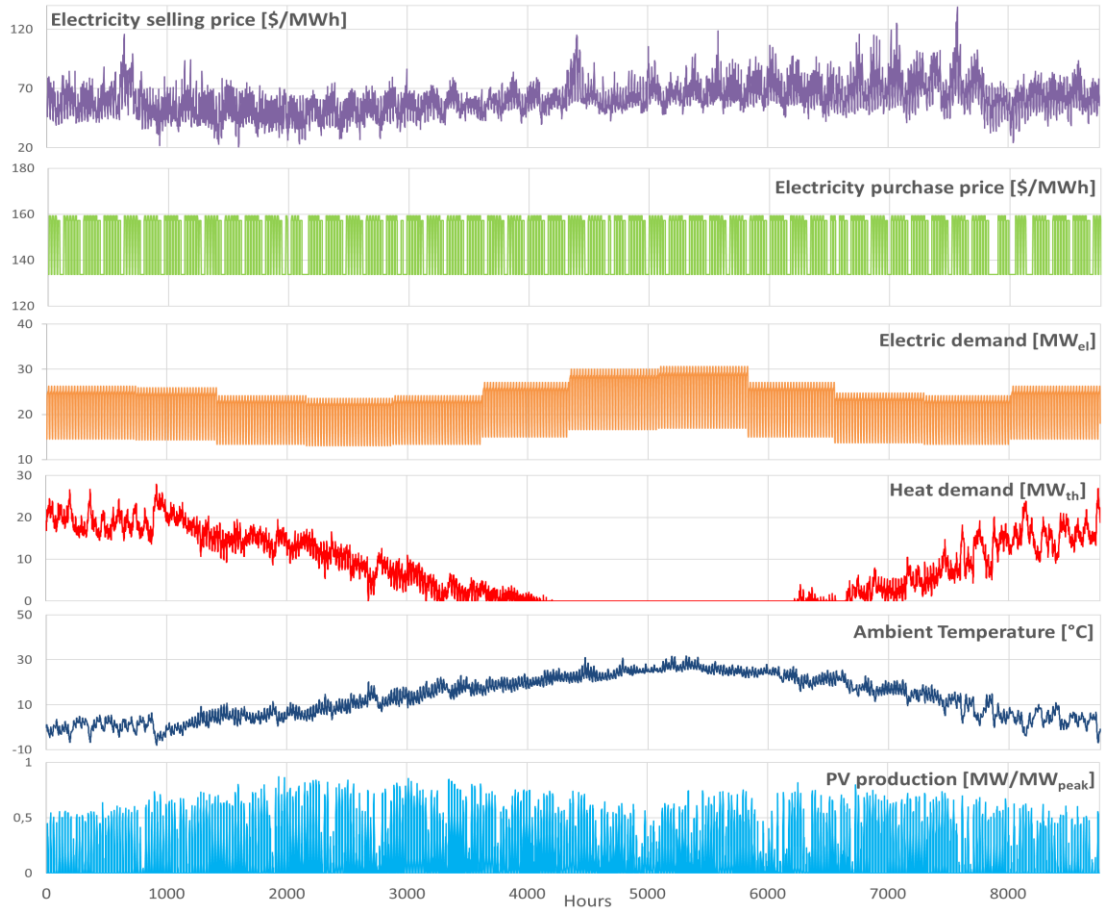

Figure 2. *Representation of the time-variable yearly input profiles considered in this study.*

All gas turbines in the model are arranged in the combined heat and power (CHP) asset, with heat recovered from the exhaust gas through a counter-current heat exchanger.
The gas turbines are modelled as single input - multiple output machines, taking natural gas from the grid as input and producing electricity, heat, and CO_2 emissions as output. To model the input/output relationship, we have considered a linear approximation that achieves high accuracy (coefficient of determination above 0.99) for gas turbine load between 100% and 50%.

The model considers the off-design behaviour of gas turbines as a function of ambient temperature. Gas turbine performance maps, which show input/output relations, are first evaluated for discrete ambient temperature values. Then, linear interpolation is carried out to determine the gas turbine performance curve for the actual ambient temperature value at each time step. An example of the performance curves is reported in Figures 3 and 4. The reported performance data are normalized for the ISO conditions at 15°C.

A convex-hull formulation is utilized to account for the input/output relationship, considering two vertexes, the maximum and minimum load condition:

$$Fuel_{input_{m,t}} = \alpha_{m,1,t} \cdot \tilde{F}_{m,1} + \alpha_{m,2,t} \cdot \tilde{F}_{m,2} \quad (2)$$

$$P_{m,t} = \alpha_{m,1,t} \cdot \tilde{P}_{m,1} + \alpha_{m,2,t} \cdot \tilde{P}_{m,2} \quad (3)$$

$$Q_{m,t} = \alpha_{m,1,t} \cdot \tilde{Q}_{m,1} + \alpha_{m,2,t} \cdot \tilde{Q}_{m,2} \quad (4)$$

$$z^{on}_{m,t} = \alpha_{m,1,t} + \alpha_{m,2,t} \quad (5)$$

Where $Fuel_{input_{m,t}}$ is the fuel input of the machine m at time t. $\alpha_{m,v,t}$ is the variable that estabilishes the load of the machine m at time t for the vertex v. $\tilde{F}_{m,1}$, $\tilde{P}_{m,v}$, and $\tilde{Q}_{m,v}$ represent the vertex value of fuel input F, electric power P and thermal power Q for the machine m, respectively. Similarly, $P_{m,t}$ and $Q_{m,t}$ are the electric power and thermal power output of the machine m at time t. $z^{on}_{m,t}$ is the binary variable which represent the commitment status (1 if turned-on, 0 if turned-off) of the machine m at time t. Lastly, the gas turbines are modelled as fast machines without start-up/shut-down or ramp-up/ramp-down limitations. To provide a rough idea of the considered gas turbines, some input data are approximated in Table 1, in p.u. with respect to a base case selected to be characterized by about 40 MW of nominal electrical and thermal output power (about 50% of the considered electrical load peak), 40% of efficiency, 20 M$ of capital investment cost, 300 $/h of O&M variable cost and 3000 $/start-up of start-up costs. Since the focus of the paper is describing the approach based

on optimization, approximated data are shown for reference only. The MILP model can optimize the number and the technology of the gas turbines to be installed. Mixed technology solutions are also allowed.

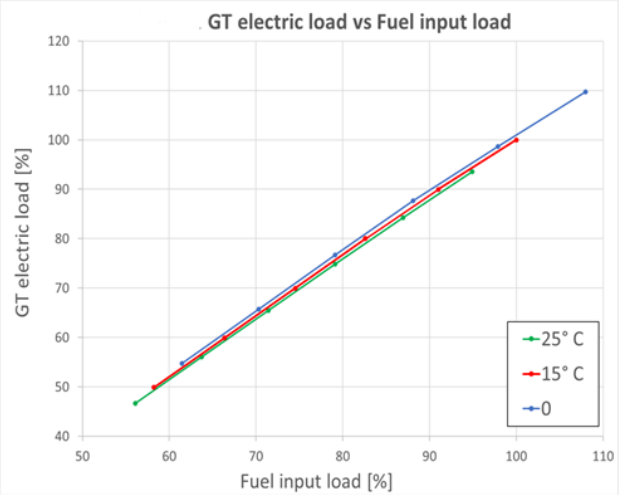

Figure 3. Electric load as a function of the fuel load.

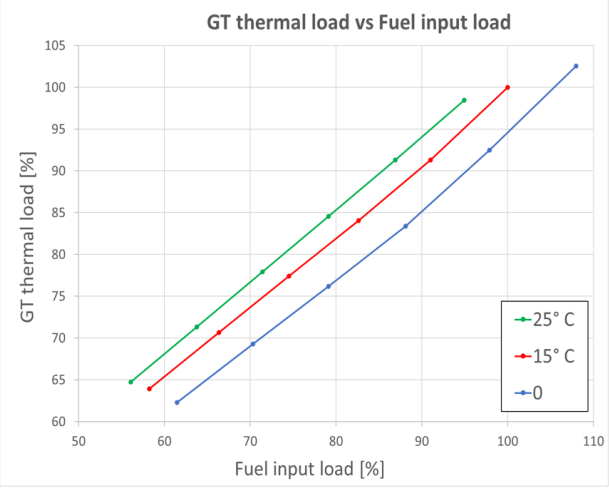

Figure 4. *Cogenerated thermal load as a function of the fuel load.*

Heat Pump

In the machine catalogue for thermal power production, a variable-size heat pump has been included, with a nominal output of 35 MW_{th} and a COP of 3.5 at full load. The heat pump model is a single input - single output machine that uses electricity to generate heat. The performance curve for the heat pump at variable load is obtained from De Pasquale et al. (2016), assuming a linear relationship between electric input and thermal power output. An off-design behaviour, which varies with temperature, is also considered, based on the producer datasheet. Furthermore, the heat pump can be optimally sized from 1 to 10 MWe. The input/output relation is again modelled with a convex-hull formulation. This is reported by Zatti et al. (2019a), who extended the formulation of equations 2-5 for variable-size machines, considering the effect of the size on the machine efficiency. The investment cost is calculated using Equation 6 (Pieper et al., 2018), while the start-up cost is set to $40 \cdot Size_{input}$ \$/start-up. Additionally, an extra electricity consumption per start-up of $0.12 \cdot Size_{input}$ %/start-up is considered.

$$Cost_{HP} = 2.239 \cdot Size_{input} + 0.505\ [M\$] \quad (6)$$

PV fields

Among the non-dispatchable units, the study includes three PV fields, each with a maximum capacity of 80 MW. The division into three fields has been employed to improve the reliability: in case of failure of one PV field, it can be backed-up by the spinning reserve and spare generator. The PV technology adopted is crystalline silicon with a nominal efficiency of 19%. The SAM software was used to simulate the PV system using weather data from Incheon Airport in 2019. The input/output relationship is governed by the following equation:

$$Out\_PV_t = P\_PV_t \cdot Size_{PV} \quad (7)$$

Where P_PV_t is the power of the PV field per unit size derived from the profiles at time t. $Size_{PV}$ is the variable that represents the size of the PV field in MW. Out_PV_t is the power generated by the PV field at time t.

Economic data include a specific capital investment cost of 841.2 \$/kW installed and O&M costs of 13.06 \$/MWp-year (IEA, 2020).

Battery and thermal energy storage systems

The model includes two types of storage systems: battery energy storage (BESS) and thermal energy storage (TES). In the case of BESS, four modules are installed to enhance the system's reliability. In fact, BESS is considered essential for providing the spinning reserve, since it reacts instantaneously to a system failure and also serves as a power bank. The performance and economic data for both storage technologies, which are taken from Castelli et al. (2022) and Zatti et al. (2019a) are presented in Table 2.
The storage systems are modelled according to the following energy balances:

$$SOC_{es,t} = SOC_{es,t-1} \cdot \tilde{\eta}_{es}^{sd} + \left(P_{es,t}^{ch} \cdot \tilde{\eta}_{es}^{ch} - P_{es,t}^{disch} \cdot \tilde{\eta}_{es}^{disch}\right) \cdot \Delta t \quad (8)$$

Where $SOC_{es,t}$ is the state-of-charge of the storage es at time t. $P_{es,t}^{ch}$ and $P_{es,t}^{disch}$ represent the charge and discharge power of the storage es at time t, respectively.

Problem constraints

A detailed illustration of the constraints utilized in the MILP model is not reported in this work but is instead available in the prior works of Politecnico di Milano (Zatti et al., 2019a), (Zatti et al., 2017).

Table 1. *Approximate performance and economic input data of the gas turbine models employed in this study.*

GT Model	GTurbA	GTurbB	GTurbC	GTurbD	GTurbE
Nominal P_{el} [p.u.]	1.0	0.8	0.4	0.3	0.15
Nominal η_{el} [%]	40	38	35	34	30
Nominal P_{th} [p.u.]	1.0	0.95	0.55	0.45	0.25
Capital investment cost [p.u.]	1.0	0.75	0.5	0.45	0.3
O&M variable cost [p.u.]	1.0	0.7	0.5	0.4	0.25
Start-up cost [p.u.]	1.0	0.7	0.5	0.4	0.25

Table 2. *Input data of storage systems.*

Technology	BESS module	TES
Size range [MWh]	0-20	0-50
C-rate [1/h]	1	1
Charge efficiency ($\tilde{\eta}_{es}^{ch}$) [%]	95	85
Discharge efficiency ($\tilde{\eta}_{es}^{disch}$)[%]	95	85
Self-discharge efficiency ($\tilde{\eta}_{es}^{sd}$) [%]	99.995	95
Specific investment cost [$/kWh]	420.61	21.03
O&M variable cost [$/kWh]	0.0841	0

Specific reliability constraints have been included in the model to ensure a reliable operation with N-1 redundancy. In particular, the system must be designed and operated meeting the following class of reliability constraints:

a) Instantaneous spinning reserve: in case of failure of one generator or PV field or BESS module, the inertia of the failing unit must be met by the inertia of the running gas turbines (here called "GT allowance") and the battery. The GT allowance is set to 25% of the GT nominal power as a first guess, while the battery is assumed to react instantaneously.
b) Reserve constraint: in the 30 minutes subsequent the failure, the power of the failing unit must be taken by ramping-up the dispatchable generators ("upward reserve") and/or discharging the battery. As a safety margin, the reserve power which can be provided by the battery is computed considering the current state of charge and a discharge time horizon of 30 minutes. Furthermore, the upward reserve needs to compensate also sudden fluctuations in PV (-20%) and electric power demand (+10%).
c) Spare unit: in case of failure, the AES requires a spare gas turbine to be turned on and re-establish the N-1 reserve. The spare gas turbine takes approximately 30 minutes to start-up and reach minimum load. The selection of the spare generator is optimized by choosing from the available gas turbines in the catalogue while guaranteeing that the spare generator size is sufficiently large to replace the failing unit.

All these constraints are formulated as mixed integer linear constraints and included into the AES optimization code.

Modelling of the EV smart charging station

This work presents a methodology for modelling electric vehicles in a microgrid with a smart charging approach and optimal sizing of the charging station. The MILP model considers the electrical demand of EVs as an adjustable demand that can be optimally scheduled (Balasubramaniam et al., 2016). The EVs' yearly time-variable arrival and departure profiles are computed based on Incheon Airport's actual arrival and departure profiles. To simulate the number of EVs per passenger, a ratio of 0.3 is assumed, while the proportion of EVs in the total number of cars is assumed to be 0.1, based on the projections for 2030 in China (IEA, 2021a).

The model treats each electric vehicle as a battery with an initial average state of charge of 20%, which needs to be fully charged within a maximum parking time of 24 hours, assuming an average battery capacity of 70 kWh. Moreover, the state of charge of the EVs can only increase, as the vehicle-to-grid (V2G) approach is not considered in this work. To make the model more realistic, a random distribution of the departure profiles of the EVs in each fleet has been imposed, while still respecting the overall departure profiles from the parking lot.

Overall, the total power that is delivered to the charging station at each timestep, which is also added to the energy and power balance constraints, is limited by the EV's maximum energy level in the parking lot. In the final step, the size of the charging station is determined by selecting the highest power value delivered to the station across all timesteps. The cost associated with constructing the charging station is included in the objective function as an investment cost, which assumes a standard charger size of 19.2 kW and a cost of 2.2 k$ (Khaksari et al., 2021). As a result, the size of the charging station is optimized to minimize overall costs.

RESULTS

The optimization problem for the aggregated energy system serving the airport was solved using the Pyomo environment and Gurobi (one of the most efficient MILP

solvers (Gurobi Optimization, 2023)). The problem was formulated with a relative MIP gap of 0.5%.

The performance of the AES is optimized under two different conditions: (i) an off-grid scenario, where the microgrid must fully satisfy the electrical and thermal demand of the airport and the charging station while complying with reliability constraints; (ii) an on-grid scenario, where the AES can buy and sell electricity with the electrical grid based on market prices. Reliability constraints are not included as electricity can be imported from the grid in case of unit failure. The natural gas price was set to 5.5 $/GJ, reflecting a medium European price before 2020. Additionally, a Carbon tax value of 50 $/ton was considered in both scenarios. The results are compared to a reference non-optimized scenario in which the electricity is entirely purchased from the grid and the thermal demand is met by a boiler sized on the demand peak.

Off-grid case:

The optimized aggregated energy system in the off-grid scenario is characterized by the following optimal design:

- Three gas turbines: 2 GTurbB operated and one installed as spare.
- PV size: 48.8 MWe, equally distributed across three PV fields.
- BESS size: 35.3 MWh, divided into four modules.
- TES size: 30 MWh.

The total annual cost of the system is estimated to be 28.18 M$/year, with the cost of electricity being 109.58 $/MWh. The optimal operation of the aggregated energy system during typical and extreme days is shown in Figure 5, which displays cumulative electric and thermal energy balance plots. The vertical dashed lines separate the different typical and extreme days. In the electric energy balance plot, the black line represents the electric demand of the airport, while the blue line shows the total electricity produced for the airport and the charging station.

The optimal design solution features only the GTurbB since it is characterized by the lowest specific investment cost (about 450 $/kWel) and one of the highest efficiencies among the gas turbines in the catalogue. The first GTurbB (GT-1) operates for 7784 hours during the year, with an average load of 72%. On the other hand, the second GTurbB (GT-2) is used only during the extreme day in which the electric demand peaks at 60 MWe. The spare gas turbine is never turned on. Moreover, the yearly gas turbine electric production is approximately 67% of 257.15 GWh, as shown in Table 3.

Despite having a lower cost of electricity (66.2 $/MWh) than the GTurbB gas turbine (108.8 $/MWh), the amount of PV installed in the AES system is relatively low due to several factors. Firstly, the installation of PV is limited by reliability constraints because the technology lacks a proper energy reserve like gas turbines and batteries and requires additional spinning reserves due to the uncertainty in production forecasts.

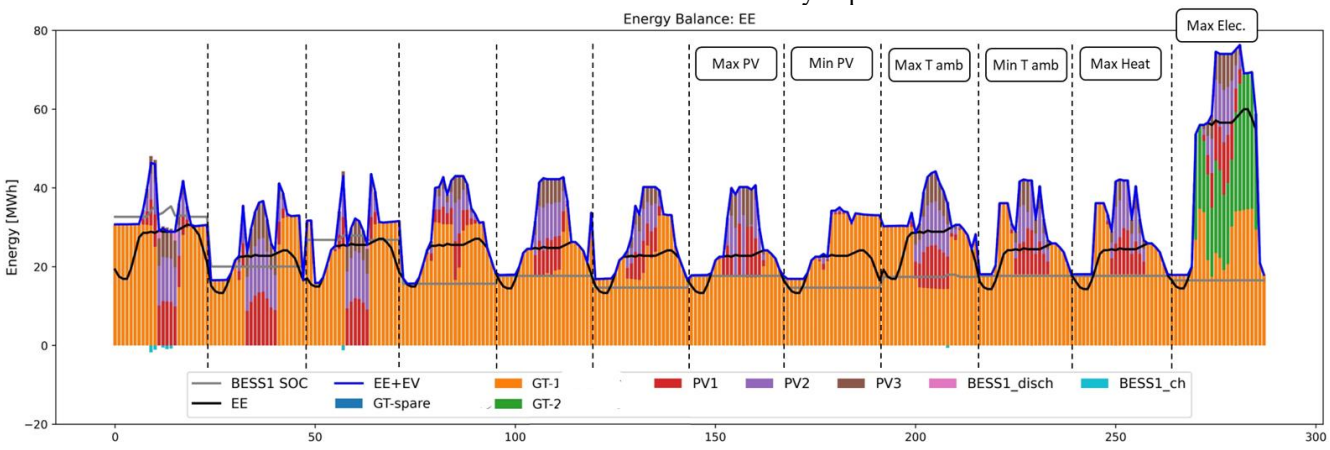

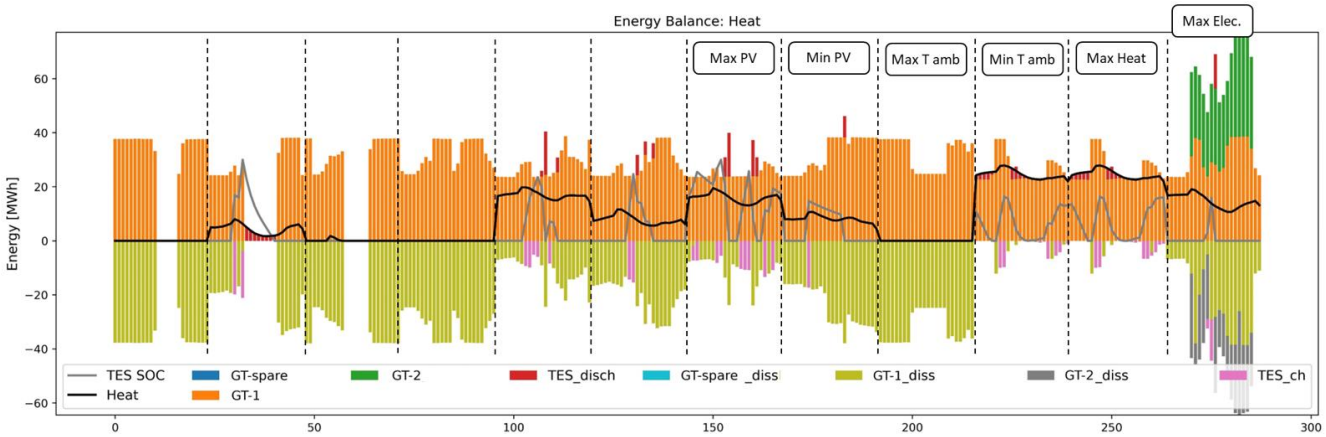

Figure 5. *Electrical and thermal cumulative energy balance on the six typical and six extreme days for the off-grid case.*

Secondly, an increase in PV production would decrease the load on the gas turbine, leading to a decrease in efficiency and, hence, a rise in fuel consumption. Thirdly, the system PV plus BESS can not substitute the gas turbines, having a higher cost of electricity. Finally, a decrease in gas turbine load or switching off of the turbine would impact the thermal power balance, potentially requiring the installation of a heat pump or larger thermal energy storage system to maintain balance, which increases costs. Therefore, PV production, which is never curtailed during the year, is exploited mainly to charge electric vehicles during the central hours of the day and accounts for about 33% of the yearly electric production. Only in the first three typical days, the gas turbines are all turned off, and the entire electric production of the AES is due to the PV. During these hours, it can also be noted from the thermal energy balance that the heat demand is null or relatively low.

The battery energy storage system has as a power bank function, covering the gas turbine and PV in the event of failure. It is only slightly discharged to meet electrical demand on the first and third typical days.

Based on the thermal energy balance, the thermal demand is almost entirely met by the thermal energy that is cogenerated by the gas turbines. To fulfil the demand, a thermal energy storage is installed instead of the heat pump, due to the lower specific cost and better integration with the CHP gas turbines. The TES is only utilized on the second typical day and during the extreme day with the highest thermal demand.

In terms of EV charging, the optimized design features 910 EV chargers. Consequently, the maximum power supplied to the EVs, which is used to size the charging station, reaches 17.47 MW. This value is greater than the maximum power that would be required for a non-flexible solution in which the EVs are instantly charged as they arrive (16.1 MW). Thus, it is more cost-effective to exploit the low cost of electricity of the PV to charge the EVs instead of peak shaving, an operation that would reduce the power needed at peak demand times and, therefore, the investment cost of the charging station.

On-grid case:

In the grid-connected scenario, the AES is optimized with a design that includes:

- One GTurb2 gas turbine
- PV size: 76 MWe, equally distributed across three PV fields.
- TES size: 47.4 MWh.

The design is optimized to minimize the total annual cost, considering an electricity export price from ref. (GME, 2023), while the import price is defined as a standard tariff of an average industrial user.

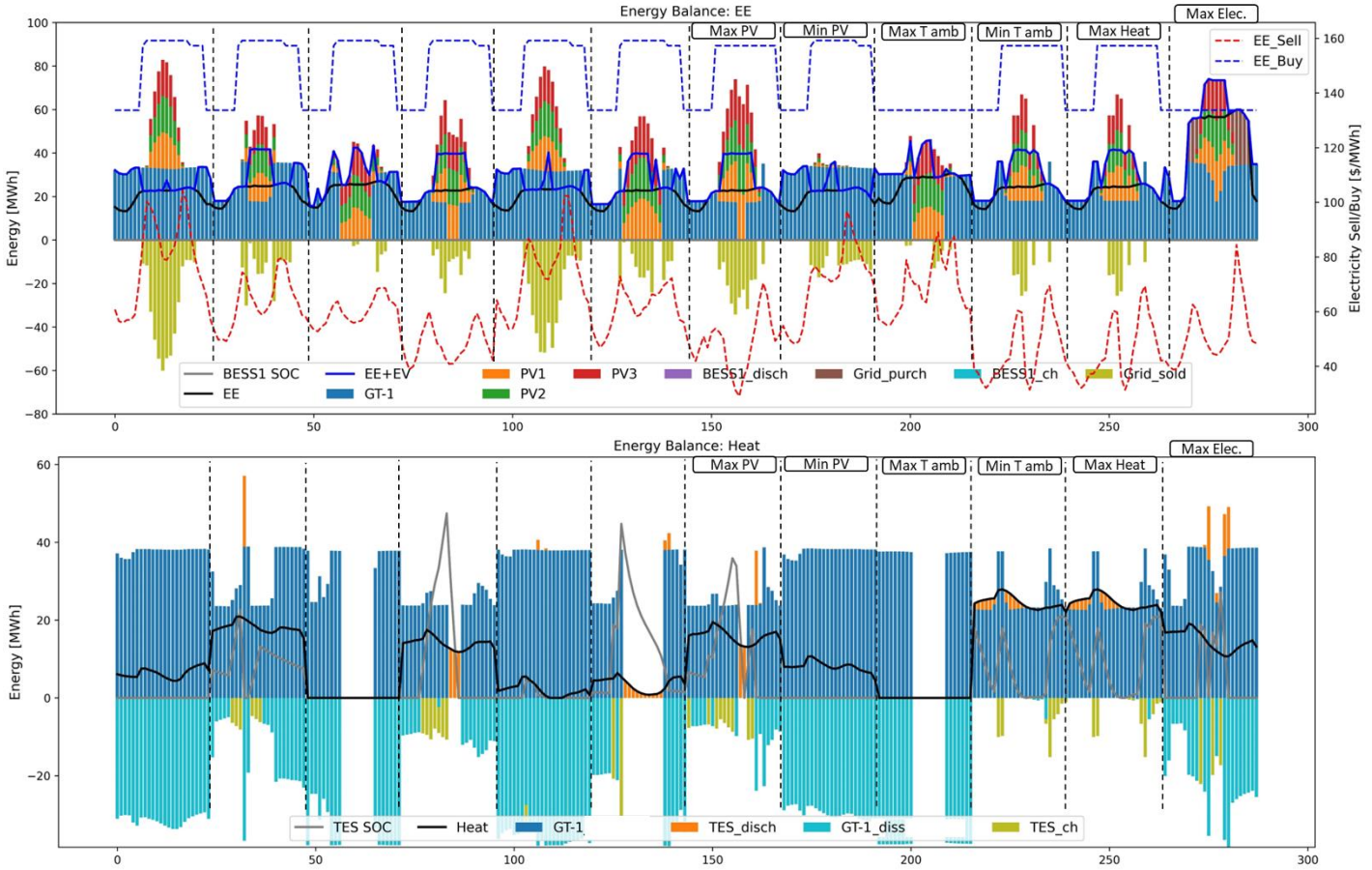

Figure 6. *Electrical and thermal cumulative energy balance on the six typical and six extreme days for the on-grid case.*

Table 3. *Main optimization global results.*

Scenario	Off-Grid	On-Grid	Reference
Optimal design	3 CHP GTurbB GT PV size: 48.8 MW BESS size: 35.3 MWh TES size: 30 MWh	1 CHP GTurbB GT PV size: 76 MW BESS size: 0 MWh TES size: 47.4 MWh	All electricity imported from the grid. Boiler size: 31 MWh
TAC [M$/y]	28.18	22.73	45.65
Yearly operational cost [M$/y]	17.91	18.29	45.49
Yearly investment cost [M$/y]	10.27	8.16	0.16
Yearly revenues [M$/y]	-	3.72	-
Electricity generated [GWh/y]	257.15	304.26	257.15
Electricity generated PV [GWh/y]	71.61	115.36	-
Electricity generated gas turbines [GWh/y]	185.54	188.90	-
Electricity to charging station [GWh/y]	59.84	59.84	59.84
Electricity exported to the grid [GWh/y]	-	53.11	-
Fuel consumption [GWh/y]	515.08	514.04	75.62
CO_2 emissions [kton/y]	101.65	101.46	116.94
Carbon Intensity [kgCO_2/MWh]	395.28	333.44	454.78

The CO_2 emissions for the grid purchased electricity are evaluated considering a carbon intensity of 400.4 kgCO_2/MWh (ISPRA, 2022). This way, the TAC includes the revenues from the electricity sold to the grid (3.72 M$/y), and it is found to be 22.73 M$/y. The corresponding cost of electricity is 74.62 $/MWh. The cumulative electrical and thermal energy balances of the grid-connected case are illustrated in Figure 6. The gas

turbine operates for 7221 hours at an average load of 78.4%, generating around 62% of the total electricity produced. The technology installed is the GTurbB for the same reasons explained for the off-grid scenario. Moreover, as the reliability constraints are not included in the problem formulation in the grid-connected case, there is no need to install a spare turbine. Utilizing a gas turbine rather than purchasing electricity from the grid is more cost-effective because of the lower COE (99.04 $/MWh). Furthermore, the use of gas turbines enables the production of thermal power to meet the airport's demand. Therefore, the electricity from the grid is only bought to meet demand peaks when the gas turbine is at maximum load and the PV is insufficient to meet the demand.

Compared to the off-grid case, a higher quantity of PV is installed, enabling the sale of excess electricity, and generating additional revenue, especially when the export price is favourable. Consequently, the PV accounts for 37.91% of the total electricity generated, representing a 5% increase compared to the previous case. In addition, there are about 1540 hours in which the gas turbine is not operating, and the PV system alone satisfies the entire electricity production, impacting the thermal energy balance.

Unlike the off-grid scenario, installing a BESS is not justified as the cost of electricity for the combined PV and battery system is higher than that of the GTurbB. Moreover, since reliability constraints are not considered in the grid-connected case, using a BESS as a power bank is no longer necessary.

The cogeneration of the gas turbine again satisfies almost the entire thermal demand. A thermal energy storage is preferred over a heat pump, similar to the off-grid case. However, the TES size is larger than in the previous scenario because the gas turbine is turned off when the thermal demand is higher.

Regarding the charging station, a total of 883 chargers have been installed, with a maximum capacity of 16.95 MW. The same considerations as in the off-grid case still apply. However, the impact of increasing the peak power delivered to the EVs to take advantage of the PV's low COE is diminished because the electricity generated by the PV is also sold to the grid.

Overall, compared to the off-grid case, the grid-connected configuration results in a lower TAC (-19.3%). The reduction is due to several factors. Firstly, the absence of reliability requirements allows for a decrease in investment costs (-20.6%), avoiding the installation of BESS and only requiring a single gas turbine. Secondly, the on-grid system allows for greater cost-effectiveness of PV as it generates revenue from exporting electricity. Additionally, the higher power generated by RES leads to a slight reduction in the fuel expenses and CO_2 emissions (i.e. carbon tax). Conversely, the increase in the investment cost for the TES and PV and the higher O&M of PV do not significantly impact the TAC.

Based on the findings presented in Table 3, it can be observed that the TAC of the reference scenario amounts to 45.65 M$/y, corresponding to a COE of 179.25 $/MWh. These results demonstrate the effectiveness of the proposed optimization methodology, as it enables a reduction in the TAC of -38.7% and -50.2% for the off-grid and grid-connected scenarios, respectively. The observed cost reductions are primarily attributed to the utilization of gas turbines, which exhibit a lower COE compared to the cost of purchasing electricity. Moreover, the optimization framework facilitates a reduction in CO_2 emissions.

CONCLUSIONS

The present study, conducted in collaboration with Baker Hughes, aims to optimize the design of an aggregated energy system for a medium-sized airport with high reliability requirements. The problem is formulated as a stochastic MILP model with the objective of minimizing the total annual cost, including both capital and operational costs. The model includes a wide range of reliability constraints (N-1 reliability, spinning reserve, etc.) and allows for the optimal sizing of the integrated charging station while scheduling the EVs' charging. The set of units available for selection includes CHP gas turbines, a heat pump, PV, BESS, and TES.

The performance of the aggregated energy system are optimized in two conditions, i.e., off-grid and grid-connected scenarios. The outcomes are compared with the reference case, where the electricity is entirely purchased from the grid. The study demonstrates that the optimized scenarios significantly reduce the total annual cost compared to the reference case (-38.7% and -50.2% for the off-grid and grid-connected cases, respectively), indicating the effectiveness of the optimization code in dealing with real-world problems.

The findings of the study demonstrate that the most efficient design for both scenarios is heavily dependent on the utilization of CHP gas turbines to produce both electric and thermal power.

The grid-connected configuration yields a lower total annual cost (-19.3%) than the off-grid case primarily due to the absence of reliability requirements, which leads to a decrease in the investment cost, and the opportunity to export electricity generated with PV.

REFERENCES

Baek, S., Kim, H., & Chang, H. J. (2016). Optimal hybrid renewable airport power system: Empirical study on Incheon International Airport, South Korea. *Sustainability (Switzerland)*, *8*(6). https://doi.org/10.3390/su8060562

Balasubramaniam, K., Saraf, P., Hazra, P., Hadidi, R., & Makram, E. (2016). A MILP Formulation for Utility Scale Optimal Demand Side Response. *IEEE Power and Energy Society General Meeting (PESGM)*, 1–5. https://ieeexplore.ieee.org/stamp/stamp.jsp?tp=&arnumber=7741956

Castelli, A. F., Pilotti, L., & Martelli, E. (2022, June 13). Optimal Design and Operation Planning of VPPs Based on Hydrogen Storage and Hydrogen Combined Cycle. *ASME Turbo Expo; Cycle Innovations: Energy Storage*. https://doi.org/10.1115/GT2022-82609

De Pasquale, A. M., Giostri, A., Romano, M. C., Chiesa, P., Demeco, T., & Tani, S. (2016). *District heating by drinking water heat pump: Modelling and energy analysis of a case study in the city of Milan*. https://doi.org/10.1016/j.energy.2016.12.014

Gabrielli, P., Gazzani, M., Martelli, E., & Mazzotti, M. (2018). Optimal design of multi-energy systems with seasonal storage. *Applied Energy*, *219*, 408–424. https://doi.org/10.1016/j.apenergy.2017.07.142

GME. (2023). *Dati - MGP prezzi*. Https://Www.Mercatoelettrico.Org/It/Default.Aspx.

Gurobi Optimization, L. (2023). *Gurobi Optimizer Reference Manual*.

IEA. (2017). *Digitalization & Energy*. www.iea.org/t&c/

IEA. (2020). *World Energy Outlook 2020*. www.iea.org/weo

IEA. (2021a). *Global EV Outlook 2021 Accelerating ambitions despite the pandemic*. www.iea.org/t&c/

IEA. (2021b). *Net Zero by 2050 - A Roadmap for the Global Energy Sector*. www.iea.org/t&c/

ISPRA. (2022). *Indicatori di efficienza e decarbonizzazione del sistema energetico nazionale e del settore elettrico*. www.isprambiente.gov.it

Khaksari, A., Tsaousoglou, G., Makris, P., Steriotis, K., Efthymiopoulos, N., & Varvarigos, E. (2021). Sizing of electric vehicle charging stations with smart charging capabilities and quality of service requirements. *Sustainable Cities and Society*, *70*. https://doi.org/10.1016/j.scs.2021.102872

National Renewable Energy Laboratory. (2020). *System Advisor Model*.

Pieper, H., Ommen, T., Buhler, F., Lava Paaske, B., Elmegaard, B., & Brix Markussen, W. (2018). Allocation of investment costs for large-scale heat pumps supplying district heating. *Energy Procedia*, *147*, 358–367. https://doi.org/10.1016/j.egypro.2018.07.104

Zatti, M., Gabba, M., Freschini, M., Rossi, M., Gambarotta, A., Morini, M., & Martelli, E. (2019). k-MILP: A novel clustering approach to select typical and extreme days for multi-energy systems design optimization. *Energy*, *181*, 1051–1063. https://doi.org/10.1016/j.energy.2019.05.044

Zatti, M., Martelli, E., & Amaldi, E. (2017). A three-stage stochastic optimization model for the design of smart energy districts under uncertainty. *Computer Aided Chemical Engineering*, *40*, 2389–2394. *https://doi.org/10.1016/B978-0-444-63965-3.50400-1*

Zatti, M., Martelli, E., & Consonni, S. (2019). *Optimal design of urban energy districts under uncertainty* [PhD Thesis, Politecnico di Milano]. www.leap.polimi.it